NASA TECHNICAL NOTE

NASA TN D-7660

NASA TN D-7660

EVALUATION OF MAGNETIC REFOCUSING IN LINEAR-BEAM MICROWAVE TUBES

by N. Stankiewicz

Lewis Research Center
Cleveland, Ohio 44135

NATIONAL AERONAUTICS AND SPACE ADMINISTRATION • WASHINGTON, D. C. • MAY 1974

1. Report No.	2. Government Accession No.	3. Recipient's Catalog No.
NASA TN D-7660		

4. Title and Subtitle	5. Report Date
EVALUATION OF MAGNETIC REFOCUSING IN LINEAR-BEAM MICROWAVE TUBES	MAY 1974
	6. Performing Organization Code

7. Author(s)	8. Performing Organization Report No.
N. Stankiewicz	E-7826
	10. Work Unit No. 502-23

9. Performing Organization Name and Address	11. Contract or Grant No.
Lewis Research Center National Aeronautics and Space Administration Cleveland, Ohio 44135	
	13. Type of Report and Period Covered: Technical Note

12. Sponsoring Agency Name and Address	14. Sponsoring Agency Code
National Aeronautics and Space Administration Washington, D.C. 20546	

15. Supplementary Notes

16. Abstract

Magnetic field configurations in which the axial component of the field decays linearly to a constant plateau field are evaluated for use in refocusing the output beam of linear beam microwave tubes. The slope of the decay and the value of the plateau field are parameters in this study. Expansion of the beam in a decaying magnetic field with subsequent dilution of space charge forces and reduction of transverse velocities is essential for efficient collection of the spent electrons. A uniform beam with a space charge force only in the radial direction is assumed, and the electron trajectories are computed for various classes. Each class is characterized by an energy and an injection angle. For a given magnetic configuration (slope and plateau value) the plateau length is calculated for a specified class and the rms deviation of the output angles for all classes is computed at the end of this plateau length. A minimum condition for a refocused beam is defined to be one in which the rms value of the output angles is less than the rms input. Many of the configurations satisfied this criteria and successfully reduced the rms value by half. However, the results are sensitive to the plateau length and an actual design should be capable of controlling this length.

17. Key Words (Suggested by Author(s))	18. Distribution Statement
Electron beams Microwave tubes Refocusing	Unclassified - unlimited Category 09

19. Security Classif. (of this report)	20. Security Classif. (of this page)	21. No. of Pages	22. Price*
Unclassified	Unclassified	31	$3.25

* For sale by the National Technical Information Service, Springfield, Virginia 22151

EVALUATION OF MAGNETIC REFOCUSING IN LINEAR-BEAM MICROWAVE TUBES

by N. Stankiewicz

Lewis Research Center

SUMMARY

Magnetic field configurations in which the axial component of the field decays linearly to a constant plateau field are evaluated for use in refocusing the output beam of linear beam microwave tubes. The slope of the decay and the value of the plateau field are parameters in this study. Expansion of the beam in a decaying magnetic field with subsequent dilution of space charge forces and reduction of transverse velocities is essential for efficient collection of the spent electrons.

A uniform beam with a space charge force only in the radial direction is assumed, and the electron trajectories are computed for various classes. Each class is characterized by an energy and an injection angle. For a given magnetic configuration (slope and plateau value) the plateau length is calculated for a specified class and the rms deviation of the output angles for all classes is computed at the end of this plateau length. A minimum condition for a refocused beam is defined to be one in which the rms value of the output angles is less than the rms input. Many of the configurations satisfied this criteria and successfully reduced the rms value by half. However, the results are sensitive to the plateau length and an actual design should be capable of controlling this length.

INTRODUCTION

A major problem in improving the efficiency of linear beam microwave tubes is the recovery of the spent beam energy. Some early schemes used one- or two-stage depressed collectors in which the electrons would give up their energy by doing work against the electrostatic potential of a collector plate. These early designs (discussed by Kosmahl in ref. 1) of Wolkstein (ref. 2) and Sterzer (ref. 3) have three primary defects.

First, these collectors are efficient in collecting electrons of only one or two energy classes. Electrons having energies higher than the potential "hill" of the collector

dissipate their excess energy as heat. However, electrons with insufficient energy to climb the hill present a backstreaming problem because they can be reflected back into the rf interaction region causing noise. Second, the metallic boundaries of these early collectors did not coincide with natural equipotential surfaces. This can cause strenuous deflections of the electrons even though they may have the correct energy. These violently deflected electrons can be reflected back into the tube and contribute to the noise problem. Or they might impinge upon the tube walls or onto a mismatched potential surface thereby producing results which are counter productive to collector efficiency.

Third, for efficient collection it is essential that, prior to entering the collector, the beam must be conditioned in a refocusing region to reduce space charge forces and transverse velocities. The emergent beam of a Klystron or a traveling wave tube as it leaves the rf interaction region quickly becomes debunched. The fast electron of late cycles overtake the slow electrons from previous cycles and the beam becomes homogeneous in the axial direction. However, the beam is still in a highly compressed radial state. Within the tube the strong space charge force of the beam is balanced by a confining magnetic field. At some point the magnetic field decays and eventually goes to zero resulting in an expansion of the beam. If the decay is too sudden, the beam virtually explodes making collection difficult.

Figure 1 shows the resultant expansion when the magnetic field vanishes abruptly. The beam expansion for various initial axial velocities P_z is shown in this figure (symbols are defined in appendix A), and it is assumed that the beam was formed with no magnetic flux on the cathode. With these assumptions the curve labeled Class 1 represents an ideal Brillouin expansion (see refs. 4 and 5). The data points of this curve are taken from Pierce (ref. 4) and Gewartowski and Watson (ref. 5) while the continuous curves are computed using the program written for this study.

A segmented depressed collector and refocusing technique has been proposed by Kosmahl (ref. 1) and a prototype has been built and tested at Lewis Research Center (see Kavanagh, Alexovich, and Chomos (ref. 6)). The Lewis collector has 10 segments but a system study by Dayton (ref. 7) shows that, after the sixth stage, collector efficiency is improved only about 1 percent per stage.

Each segment of the depressed collector is maintained at a potential which is determined by solving Poisson's equation together with the electron trajectory equations. The simultaneous solution of these equations is an iterative procedure the details of which can be found in a report by Reese (ref. 8). A 12-gigahertz coupled cavity traveling wave tube (TWT) equipped with the Lewis designed collector and refocuser has demonstrated a dramatic increase in overall efficiency from 27 to 56 percent. The collector efficiency was determined to be 81 percent (ref. 9). This tube will be flown in the Communication Technology Satellite (CTS) about 1975. The purpose of the study is to evaluate refocusing magnetic field configurations in which the field decays linearly to a constant field. Kosmahl

(ref. 10) has proposed this technique for refocusing, decompressing, and conditioning spent electron beams before injection into a segmented depressed collector. His proposal consisted of a region of decaying magnetic field over a length of between one to three cyclotron wavelengths (computed at the main magnetic field of the tube) followed by a stabilizing region not greater than one cyclotron wavelength (computed at the plateau field). This criteria does not provide a specific optimum design but represents limiting bounds to the dimensions of the refocusing region in which the optimum is located. Branch and Neugebauer (ref. 11) evaluated several magnetic designs following the Kosmahl criteria. They concluded that the optimum design was a decay length between two to three cyclotron wavelengths followed by a plateau field of 0.6 to 0.8 cyclotron wavelengths (at the reduced field amplitude). These results will be discussed in a later section. The basic design considered in this study (see fig. 2) is a region in which the beam is allowed to expand in a linearly decaying magnetic field. This is followed by a plateau or constant magnetic field region in which the beam is stabilized at a new radius. The final radius of the beam is determined by the value of the magnetic field in the plateau region. The slope and the magnitude of the plateau region are parameters in the study. The length of the plateau region is computed.

ASSUMPTIONS

This study is intended to give a relative evaluation of the two-parameter magnetic field configuration described in the introduction. It is, therefore, required to compute a large number of cases in as short a time as possible. To facilitate matters, the following space charge assumptions are made:

(1) The beam has cylindrical symmetry and space charge forces in the axial direction are ignored.

(2) The initial radius of the beam is one Brillouin radius; a particle at a radius larger than one Brillouin radius sees a logarithmic potential.

(3) The beam is uniform in density; a particle at a radius smaller than one Brillouin radius sees a potential proportional to its radius.

These assumptions uncouple the equations of motion of the many-body problem and replace them with an equation of motion of a single particle in a cumulative potential. As the beam expands in the refocusing region, this description becomes more correct, that is, the uncoupling of particles becomes more complete.

METHOD OF SOLUTION

A class is defined in this report as those electrons having the same initial injection angle and axial velocity. At first let us limit the discussion temporarily to a beam having just one class of electrons.

As the magnetic field decays from its maximum value within the tube to a particular plateau level, the beam will expand because of space charge forces. Inertia will cause an overexpansion of the beam. In the region of the magnetic plateau the beam expansion slows as a function of the time spent in the field. At some point its radial velocity will vanish and this integration distance is the length of the plateau region. Beyond this length it is assumed that magnetic shields will effectively cause the field to vanish suddenly. This is the entrance to the collector region and the analysis could proceed as in reference 8. The design is uniquely and simply solved for a single class of electrons. However, realistic beams contain many classes of electrons and each class requires a different plateau length.

Nine classes of electrons are considered in this study; that is, three initial injection angles for each of three initial axial velocities. The three velocities are the maximum, the dc, and the minimum velocities of a beam. The initial injection angles are zero and ± the maximum injection angle. After the plateau length is determined by choosing a design class, the equations of motion of the other classes are integrated using the same magnetic configuration. The electrons arrive at the end of the plateau with a variety of angles, and those of the design class will, of course, be zero. The angular spread, the average angle, and the rms deviation are computed. A minimum requirement for a given refocusing scheme should be that the final rms deviation is less than or at least equal to the initial rms deviation of the injection angles.

RESULTS

An extensive library of cases has been computed for this study. The cases are divided into those having a cathode magnetic flux of 0.1 (almost Brillouin) and those with a cathode magnetic flux of 0.9 (nearly fully confined).

In general the results demonstrate an approach to be used in achieving a satisfactory magnetic configuration rather than a specific design even though certain of the configurations are considered superior. The reason is that the results are sensitive to small changes in the parameters which determine the trajectories. Small changes in the initial conditions, the slope of the magnetic decay, the magnitude of the plateau field or its length cause large changes in the results.

Figure 3 shows a typical set of trajectories that are computed in this study. The magnetic configuration shown on this plot has a decay slope of (1 - 0.19)/8, that is, the magnetic field decays from 1 B_o to 0.19 B_o in an axial distance of 8 a_o (approximately 1.25 λ_c). The plateau length is 20 a_o, and the design velocity is $P_{\zeta o} = 1.0$. Note that the angle of the design velocity trajectory is near zero at $\zeta = 28$ a_o. The rms value of the exit angle for all classes is computed at this point and this result represents a typical calculation for a single point in figure 4.

As mentioned in the INTRODUCTION, Branch and Neugebauer (ref. 10) evaluated designs of the type examined in the present study. They considered much broader ranges of injection energy but limited their study to 40 configurations. Their evaluation of refocusing designs were also carried out as a function of an electron distribution function.

In contrast, the present study evaluated 480 magnetic configurations and concentrated on the two parameters: decay slope and plateau field. The energies ranged from approximately 50 to 120 percent of the dc energy (i.e., $0.7 \leq P_{\zeta o} \leq 1.1$), and the injection angles were $\pm 5^o$. This study is, therefore, more appropriate to TWT spent beam refocusing. Because the equations of motion were uncoupled by use of an approximation for the space charge, both studies (ref. 10 and this study) are independent of the distribution function except as an indicator of the design minimums and maximums.

As the magnetic field decays, the particles seek new equilibrium positions in which the magnetic field balances the space charge. The inertia of the particles causes overshooting and oscillatory motion occurs. The particles with slower axial velocities oscillate most violently because they rarely find themselves in a comfortable magnetic field. An ideal decay would be one in which all particles expand monotonically. Such a design would entail a rapid magnetic decay in order to accommodate the slower particle, followed by a plateau of sufficient length to reduce the final angles.

The oscillation problem is alleviated somewhat if the plateau length is determined by the slow particles. This is shown by comparing figures 4(a) and (b) with figures 4(c) and (d). In the first two figures the plateau length was determined by the particles initially having a dc velocity ($P_\zeta = 1.0$). The second two figures were computed using the same initial conditions but a design velocity of $P_\zeta = 0.7$ was used to compute the plateau length. In all cases the beam is better focused if the plateau length is computed by using the slower velocity as the designing velocity. On the other hand, the problem is aggravated if the plateau length is determined by the fast electrons, because in this case not only would the slow electron trajectories oscillate but the dc class would also begin oscillations.

Figure 5 shows the magnetic field plateau value plotted against the axial distance ζ. The cathode field in figure 5(a) is 0.1 B_o, and in figure 5(b) it is 0.9 B_o. In both figures the design velocity is 0.7. These figures show that the Kosmahl criteria (ref. 11) is a good indication of the length of the refocusing region. These figures give the length

of the refocusing region. For example, referring to figure 4(c), we see that a minimum rms value occurs for an E-slope at a plateau magnetic field $B_p = 0.31\ B_o$. In figure 5(a) the straight lines A to F represent the linear decay of the magnetic field from a value of 1 to the plateau value B_p. In the example stated, if the slope designated as E is followed down to $B_p = 0.31\ B_o$, an axial distance of 16.6 is read. This represents the beginning of the plateau region and is 2.64 cyclotron wavelengths λ_c from the beginning of the magnetic field decay. The total length of the plateau is determined by continuing the line $B_p = 0.31\ B_o$ until it intersects with the curved line designated by E_1. The intersection occurs at an axial distance of 25 a_o. The plateau length in units of the local cyclotron wavelength (i.e., λ_c calculated at $B = 0.31\ B_o$) is 0.414 λ_c'.

The computed results demonstrate that the tuning capability should be placed on the plateau length probably by employing effective shields. The magnitude of the plateau field is best determined from the desired output radius of the beam (see fig. 6). The slope of the magnetic field decay is probably the least controllable parameter. Its value is fixed by the physical considerations of the placement and size of the iron pole piece and coil or permanent magnets.

It is noted that the magnetic configurations in this study are independent of the electron distribution function. That is, no weighting function is assigned to the classes of electrons that are considered. If it is known that most of the recoverable energy of the spent beam is carried by the fast electrons it would be advantageous to use these electrons as the design class. Because the fast electrons must penetrate most deeply into the collector it is necessary that they enter with the smallest possible radial velocity.

CONCLUSIONS

This report evaluates an extensive number of refocusing configurations of the type having a linear magnetic decay followed by a constant plateau field. The slope of the decay and the magnitude of the plateau field are parameters in this study. The electron trajectories are computed for various initial conditions; the plateau length and the exit angles of the particles are determined. The following conclusions are made:

1. A large number of possible designs exist; there is no obvious optimum design.

2. The slope of the magnetic decay should be determined by factors such as the size and availability of magnets and the general ability of the main magnetic circuit to give a linear decay.

3. The field strength of the plateau region is best determined by factors such as the desired final beam size and possible impingement problems.

4. Because of the sensitivity of the results to small changes in initial conditions and to slight changes in plateau length, it is necessary to allow for a tuning capability in any actual design.

5. The best tuning capability is control of the plateau length.

Lewis Research Center,
National Aeronautics and Space Administration,
Cleveland, Ohio, February 1, 1974,
502-23.

APPENDIX A

SYMBOLS

$\vec{A}$	vector potential
A_φ	φ component of vector potential
a_o	tunnel radius
$\vec{B}$	magnetic field
B_c	cathode field
B_o	containment field within tube; axial component
B_p	plateau magnetic field; axial component
B_z	z component of magnetic field
B_c^*	normalized cathode field
B_ζ^*	normalized magnetic field in ζ direction
b	beam radius
b^*	normalized beam radius; Brillouin radius
c_o, c_{2k}	expansion coefficients used in eq. (C30)
$\vec{E}$	electric field
e	electronic charge
H	Hamiltonian
H^*	normalized Hamiltonian
I_o	dc current
m	particle mass
P_ρ, P_ζ	normalized momenta conjugate to (ρ, ζ) coordinates
p_r, p_z, p_φ	generalized momenta conjugate to (r, z, φ) coordinates
q_e	total electron charge within volume τ
r, z, φ	cylindrical coordinates
$\hat{r}, \hat{z}$	unit vectors in r and z directions
t	time variable
u_o	dc velocity within tube

V electric potential

V^* normalized electric potential

ϵ Napierian base, 2.718...

ϵ_o dielectric constant of vacuum

ζ normalized axial direction

η electron charge to mass ratio

Θ normalized time variable

λ_c cyclotron wavelength calculation at B_o

λ_c' cyclotron wavelength calculated at B_p

ρ, ζ normalized cylindrical coordinates

ρ_e electron charge density

σ surface area

τ volume

Υ difference of magnetic flux at field point z and at cathode defined in eq. (C15), $\psi - \psi_c$

Υ^* normalized Υ function

φ angular component of cylindrical coordinates

ψ magnetic flux density

ψ_c magnetic flux density at cathode

ψ^* normalized magnetic flux density

ψ_c^* normalized magnetic flux density at cathode

ω_c cyclotron frequency

ω_p plasma frequency

Subscripts:

c cathode

e electron

o initial value

p plateau value

r radial component

z axial component

ζ axial normalized component

ρ radial normalized component

φ angular component

Superscripts:

$\hat{}$ unit vector

$\rightarrow$ vector

$*$ normalized quantity

$\cdot$ total time derivative, d/dt

APPENDIX B

ELECTROSTATIC SPACE CHARGE POTENTIAL

In evaluating the space charge effects of the beam it is assumed that there exists no z component of this force. The potential is given by Poisson's equation

$$\nabla^2 V = \frac{-\rho_e}{\epsilon_o} \tag{B1}$$

where ρ_e is the electron density distribution.

Interior Points of Beam

For interior points of the beam (i.e., $r \leq b$) the electron density is assumed to be constant and is given by

$$\rho_e = \frac{-I_o}{\pi b^2 u_o} \tag{B2}$$

where b is the beam radius, u_o is the dc velocity, and I_o is the direct current of the tube. The negative sign in equation (B2) indicates the negative charge of electrons.

Equation (B1) becomes

$$\frac{1}{r}\frac{d}{dr}\left(r\frac{dV}{dr}\right) = \frac{I_o}{\pi b^2 u_o \epsilon_o} \tag{B3}$$

This can be immediately integrated and yields

$$V = \frac{1}{4}\frac{\omega_p^2}{\eta} r^2 \qquad r \leq b \tag{B4}$$

where ω_p the plasma frequency is written as

$$\omega_p = \left(\frac{\eta I_o}{\epsilon_o u_o \pi b^2} \right)^{1/2} \tag{B5}$$

Exterior Points of Beam

For points that are exterior to the beam (i.e., $r \geq b$) Gauss' law can be used to deduce the potential. Because $\vec{E} = -\text{grad } V$, equation (B1) can be written as

$$\text{div } \vec{E} = \frac{\rho_e}{\epsilon_o} \tag{B6}$$

If equation (B6) is integrated over a cylindrical volume τ of length δz, the left side of equation (B6) can be converted to a surface integral by using Gauss' law, that is,

$$\int \text{div } \vec{E} \, d\tau = \int \vec{E} \cdot d\vec{\sigma} = 2\pi r E_r \, \delta z \tag{B7}$$

The last step in equation (B7) is possible because of the assumption that $E_z = 0$. Integrating the right side of equation (B6) over τ gives the total charge $+q_e$ within the volume $\pi b^2 \, \delta z$. Equation (B6) becomes

$$2\pi r E_r \, \delta z = \frac{q_e}{\epsilon_o} \tag{B8}$$

Using equation (B2) and the assumption of a constant density beam yields

$$q_e = \frac{-I_o}{u_o} \, \delta z$$

Solving equation (B8) for E_r gives

$$E_r = \frac{-I_o}{2\pi \epsilon_o u_o} \frac{1}{r} \tag{B10}$$

or using equation (B3) results in

$$-\frac{dV}{dr} = \frac{-I_o}{2\pi\epsilon_o u_o}\frac{1}{r} \tag{B11}$$

Integrating equation (B11) yields

$$V = \frac{I_o}{2\pi\epsilon_o u_o} \ln r + \text{constant} \tag{B12}$$

The constant in equation (B12) is evaluated by equating the potential of equation (B12) with that of equation (B4) at $r = b$. Hence,

$$V = \frac{b^2\omega_p^2}{4\eta} \ln\left[\epsilon\left(\frac{r}{b}\right)^2\right] \qquad r \geq b \tag{B13}$$

Equation (B5) was used in arriving at this form of equation (B13). The ϵ in equation (B13) is the Napierian base 2.718 . . . .

APPENDIX C

DERIVATION OF THE EQUATIONS OF MOTION

Consider a particle with charge $-e$ moving in an external axisymmetric magnetic and electric field. In cylindrical coordinates its Hamiltonian is

$$H = \frac{1}{2m}\left[p_r^2 + p_z^2 + \left(\frac{p_\varphi + erA_\varphi}{r}\right)^2\right] - eV \tag{C1}$$

In this equation p_r, p_z, and p_φ are the conjugate momenta to the cylindrical coordinates r, z, and φ. The magnetic field $\vec{B}$ is

$$\vec{B} = \text{curl } \vec{A} = \hat{r}\left(-\frac{\partial A_\varphi}{\partial z}\right) + \hat{z}\left(\frac{1}{r}\frac{\partial}{\partial r} rA_\varphi\right) \tag{C2}$$

and the electric field $\vec{E}$ is

$$\vec{E} = -\text{grad } V = -\hat{r}\frac{\partial V}{\partial r} - \hat{z}\frac{\partial V}{\partial z} \tag{C3}$$

It is possible to rewrite the vector potential in terms of the magnetic flux ψ that passes through a surface σ of perimeter s. The surface is a circle of radius r and is perpendicular to the axis z. Hence,

$$\vec{\psi} = \int \vec{B} \cdot d\vec{\sigma} = \int (\text{curl } \vec{A}) \cdot d\vec{\sigma} \tag{C4}$$

By Stokes' theorem

$$\int (\text{curl } \vec{A}) \cdot d\vec{\sigma} = \int \vec{A} \cdot d\vec{S} \tag{C5}$$

$$= \int_0^{2\pi} A_\varphi r \, d\varphi$$

$$= 2\pi r A_\varphi \tag{C6}$$

Substituting equation (C6) into equation (C4) gives

$$A_\varphi = \frac{\psi}{2\pi r} \tag{C7}$$

Because φ is a cyclic coordinate, we have

$$\frac{dp_\varphi}{dt} = \dot{p}_\varphi = -\frac{\partial H}{\partial \varphi} = 0 \tag{C8}$$

or

$$p_\varphi = \text{constant} \tag{C9}$$

This result, along with equation (C7), is used to rewrite the Hamiltonian exclusively in terms of the r and z coordinates. This emphasizes the two-dimensional character of the formulation. The second canonical equation considered is

$$\frac{\partial \varphi}{\partial t} = \dot{\varphi} = \frac{\partial H}{\partial p_\varphi} \tag{C10}$$

Performing the differentiation of equation (C1) yields

$$\dot{\varphi} = \frac{1}{m}\left(\frac{p_\varphi + erA_\varphi}{r^2}\right) \tag{C11}$$

and substituting equation (C7) into equation (C11) gives

$$\dot{\varphi} = \frac{1}{mr^2}\left(p_\varphi + \frac{e}{2\pi}\psi\right) \tag{C12}$$

The constant p_φ is evaluated from the initial condition at the cathode. If the electrons are emitted from the cathode at a radius r_c and if it is assumed that they are emitted perpendicular to the cathode (i.e., $\dot{\varphi} = 0$ at $r = r_c$), then

$$p_\varphi = -\frac{e}{2\pi}\psi_c \tag{C13}$$

and

$$\frac{1}{2m}\left(\frac{p_\varphi + erA_\varphi}{r}\right)^2 = \frac{1}{2m}\left(\frac{e\Upsilon}{2\pi r}\right)^2 \tag{C14}$$

where

$$\Upsilon = \psi - \psi_c \tag{C15}$$

The Hamiltonian (eq. (C1)) can now be written

$$H = \frac{1}{2m}\left(p_r^2 + p_z^2\right) + \frac{1}{2m}\left(\frac{e\Upsilon}{2\pi r}\right)^2 - eV \tag{C16}$$

Normalization of Equations

The variables r and z are normalized with respect to the tunnel radius a_o of the microwave tube. And the time scale t is normalized to the cyclotron frequency ω_c of the electrons. The cyclotron frequency is defined as

$$\omega_c = \frac{e}{m} B_o \tag{C17}$$

where B_o is the confinement magnetic field. Let ρ, ζ, and Θ be the normalized counterparts to r, z, and t. Hence,

$$\rho = \frac{r}{a_o}$$

$$\zeta = \frac{z}{a_o} \tag{C18}$$

$$\Theta = \omega_c t$$

The momenta are normalized to the scale factor $a_o m\omega_c$. Hence,

$$P_\rho = \frac{p_r}{a_o m\omega_c}$$

$$P_\zeta = \frac{p_z}{a_o m\omega_c} \tag{C19}$$

The magnetic field is normalized to the confinement field B_o (i.e., $B_z = B_o B_\zeta^*$) as follows:

$$\Upsilon = 2\pi\left[\int_0^r B_z(r', z')r'\,dr' - \int_0^{r_c} B_z(r', z_c)r'\,dr'\right]$$

$$= 2\pi a_o^2 B_o\left[\int_0^\rho B_\zeta^*\rho'\,d\rho' - \int_0^{\rho_c} B_\zeta^*(\rho'\zeta_c)\rho'\,d\rho'\right]$$

$$= 2\pi a_o^2 B_o\left(\psi^* - \psi_c^*\right) = 2\pi a_o^2 B_o \Upsilon^* \tag{C20}$$

The electrostatic space charge potential (see appendix B) is normalized as follows:

$$V = \frac{1}{4}\frac{a_o^2\omega_p^2}{\eta}V^* \tag{C21}$$

where

$$V^* = \begin{cases} \rho^2 & \rho \le b^* \\ (b^*)^2 \ln\left[\epsilon\left(\dfrac{\rho}{b^*}\right)^2\right] & \rho \ge b^* \end{cases} \tag{C22}$$

and

$$b^* = \frac{b}{a_o} \tag{C23}$$

These substitutions into the Hamiltonian of equation (C16) yield the normalized Hamiltonian H^*.

$$H^*\left[\rho(\Theta), \zeta(\Theta), P_\rho(\Theta), P_\zeta(\Theta)\right] = \frac{1}{\left(a_o \omega_c\right)^2 m} H\left[r(t), z(t), p_t(t), p_z(t)\right] \tag{C24}$$

$$H^* = \frac{1}{2}\left(P_\rho^2 + P_\zeta^2\right) + \frac{1}{2}\left(\frac{\Upsilon^*}{\rho}\right)^2 - \frac{1}{4}\left(\frac{\omega_p}{\omega_c}\right)^2 V^* \tag{C25}$$

The set of canonical equations gives the following set of equations of motion to be solved:

$$\frac{d\rho}{d\Theta} = \frac{\partial H^*}{\partial P_\rho} \tag{C26}$$

$$\frac{d\zeta}{d\Theta} = \frac{\partial H^*}{\partial P_\zeta} \tag{C27}$$

$$\frac{dP_\rho}{d\Theta} = -\frac{\partial H^*}{\partial \rho} \tag{C28}$$

$$\frac{dP_\zeta}{d\Theta} = -\frac{\partial H^*}{\partial \zeta} \tag{C29}$$

It is noted here that because this study is limited to a very particular magnetic field configuration, namely a linear decay followed by a constant plateau, the z component of the magnetic field has no r dependence. This is shown by considering the axial expansion formula. As shown in Gewartowski and Watson (ref. 8) a solution of the axisymmetric Laplace equation in cylindrical coordinate has the form

$$V(r, z) = \sum_{k=0}^{\infty} c_{2k}(z) r^{2k} \tag{C30}$$

in which

$$c_o = V(0, z) \tag{C31}$$

and

$$c_{2k} = \frac{(-1)^k}{2^{2k}(k!)^2} \frac{d^{2k} c_o}{dz^{2k}} \qquad k = 1, 2, \ldots \tag{C32}$$

However, in a region in which the z component of the magnetic field is a constant (i.e., $B_{zo} = -dV_o/dz$ = constant), equation (C30) reduces to

$$V(r, z) = V(0, z) \tag{C33}$$

And in a region in which $dB_{zo}/dz = -d^2V_o/dz^2$ = constant, equation (C30) reduces to

$$V(r, z) = V(0, z) - \frac{1}{4} \frac{d^2V(0, z)}{dz^2} r^2 \tag{C34}$$

Taking the z derivative of equation (C34) and inserting the proper negative sign yields

$$B_z(r, z) = B_z(0, z) \tag{C35}$$

The off-axis magnetic field B_z is equal, therefore, to the axial magnetic field. Because only the z component of the magnetic field is used in forming the magnetic flux term Υ^*, there is no need to consider the r component or its dependence on r. As a consequence, the integrations in equation (C20) can be carried out

$$\Upsilon^* = \frac{1}{2} \rho^2 B_\zeta^* - \frac{1}{2} \rho_c^2 B_c^* \tag{C36}$$

Performing the indicated partial differentiations in equations (C26) to (C28) produces the following final form of the equations of motion:

$$\frac{d\rho}{d\Theta} = P_\rho \tag{C37}$$

$$\frac{d\zeta}{d\Theta} = P_\zeta \tag{C38}$$

$$\frac{dP_\rho}{d\Theta} = -\frac{1}{4}\rho\left[\left(B_\zeta^*\right)^2 - \left(B_c^*\right)^2\left(\frac{\rho_c}{\rho}\right)^4\right] + \frac{1}{2}\left(\frac{\omega_p}{\omega_c}\right)^2 \begin{cases} \rho, & \rho \le b^* \\ \dfrac{(b^*)^2}{\rho}, & \rho \ge b^* \end{cases} \tag{C39}$$

$$\frac{dP_\zeta}{d\Theta} = -\frac{1}{4}\rho^2\left[B_\zeta^* - B_c^*\left(\frac{\rho_c}{\rho}\right)^2\right]\frac{\partial B_\zeta^*}{\partial \zeta} \tag{C40}$$

It is assumed that the radius of emissions at the cathode is equal to the beam radius, that is,

$$\rho_c = b^* \tag{C41}$$

This ignores all of the subtleties of beam formation such as thermal effects, scalloping, and other problems in electron gun design.

The parameter $\left(\omega_p/\omega_c\right)^2$ is determined from the dc conditions of the tube. A dc beam will have an equilibrium radius equal to b^* at $B_\zeta^* = 1$. Ideally the dc beam will be laminar, with no net radial forces. That is, $dP_\rho/d\Theta$ will be zero. Applying this condition to equation (C39) yields

$$-\frac{1}{4}b^*\left(1 - B_c^{*2}\right) + \frac{1}{2}\left(\frac{\omega_p}{\omega_c}\right)^2 b^* = 0$$

or

$$\left(\frac{\omega_p}{\omega_c}\right)^2 = \frac{1}{2}\left(1 - B_c^{*2}\right) \tag{C42}$$

For ideal Brillouin flow $B_c^* = 0$ and $\left(\omega_p/\omega_c\right)^2 = 1/2$.

Numerical Solution

The equations of motion (eqs. (C36) to (C39)) were integrated numerically on an IBM 7094 II Data Processing System. The program used was a revision of a program initially written for the solution of 240 coupled first-order equations. That is, the original problem contained four equations of the type shown in equations (C36) to (C39) for each of

sixty interacting particles. The coupling occurred, of course, through the space charge terms.

A simple and quick integration technique was required for the larger program in order to minimize computer time. This technique used a Taylor's series expansion of the variables ρ, ζ, P_ρ, and P_ζ, and is equivalent to a second-order Runge-Kutta integration procedure. The accuracy of the integration was checked by monitoring the total energy of the system. The energy was conserved to an accuracy of about 3 percent. The series expansion used is as follows:

$$\rho = \rho_o + \left(\frac{d\rho}{d\Theta}\right)_o \Delta\Theta + \frac{1}{2}\left(\frac{dP_\rho}{d\Theta}\right)_o (\Delta\Theta)^2 \tag{C42}$$

$$\zeta = \zeta_o + \left(\frac{d\zeta}{d\Theta}\right)_o \Delta\Theta + \frac{1}{2}\left(\frac{dP_\zeta}{d\Theta}\right)_o (\Delta\Theta)^2 \tag{C43}$$

$$P_\rho = P_{\rho o} + \left(\frac{dP_\rho}{d\Theta}\right)_o \Delta\Theta \tag{C44}$$

$$P_\zeta = P_{\zeta o} + \left(\frac{dP_\zeta}{d\Theta}\right)_o \Delta\Theta \tag{C45}$$

The step size $\Delta\Theta$ was 10^o ($\pi/18$ radians). In equations (C42) to (C45), the subscript o refers to values at the beginning of the integration step.

REFERENCES

1. Kosmahl, Henry G.: A Novel, Axisymmetric, Electrostatic Collector for Linear Beam Microwave Tubes. NASA TN D-6093, 1971.

2. Wolkstein, H. J.: Effect of Collector Potential on Efficiency of Traveling-Wave Tubes. RCA Rev., vol. 19, no. 2, June 1958, pp. 259-282.

3. Sterzer, F.: Improvement on Traveling-Wave Tube Efficiency Through Collector Potential Depression. IRE Trans. on Electron Devices, vol. ED-5, no. 4, Oct. 1958, pp. 300-305.

4. Pierce, John R.: Theory and Design of Electron Beams. Second ed., D. Van Nostrand Co., 1954, p. 202.

5. Gewartowski, James W.; and Watson, H. A.: Principles of Electron Tubes, Including Grid-Controlled Tubes, Microwave Tubes, and Gas Tubes. D. Van Nostrand Co., 1965, p. 616.

6. Kavanagh, Francis E.; Alexovich, Robert E.; and Chomos, Gerald J.: Evaluation of Novel Depressed Collector for Linear-Beam Microwave Tubes. NASA TM X-2322, 1971.

7. Dayton, James A., Jr.: System Efficiency of a Microwave Power Tube With a Multistage Depressed Collector. NASA TM X-2651, 1972.

8. Reese, Oliver, W.: Numerical Method and Fortran Program for the Solution of an Axisymmetric Electrostatic Collector Design Problem. NASA TN D-6959, 1972.

9. Kosmahl, H.; Sauseng, O.; and McNary, B. D.: A 240-W 12-GHz Space Communication TWT With 56 Percent Overall and 81 Percent Collector Efficiency. IEEE Trans. on Electron Devices, vol. ED-20, no. 12, Dec. 1973, p. 1169.

10. Kosmahl, H. G.: Electron Beam Controller. Patent No. 3,764,850, United States, Oct. 1973.

11. Branch G. M.; and Neugebauer, W.: Refocusing of the Spent Axisymmetric Beam in Klystron Tubes. NASA CR-121114, 1972.

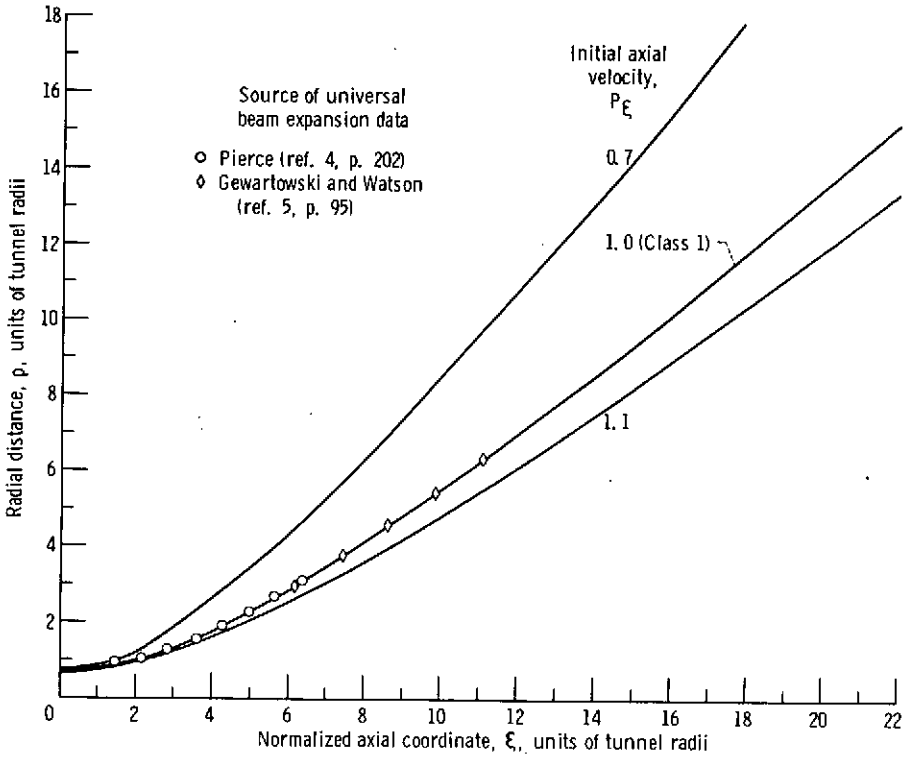

Figure 1. - Beam expansion for sudden (step function) magnetic decay for various energy classes.

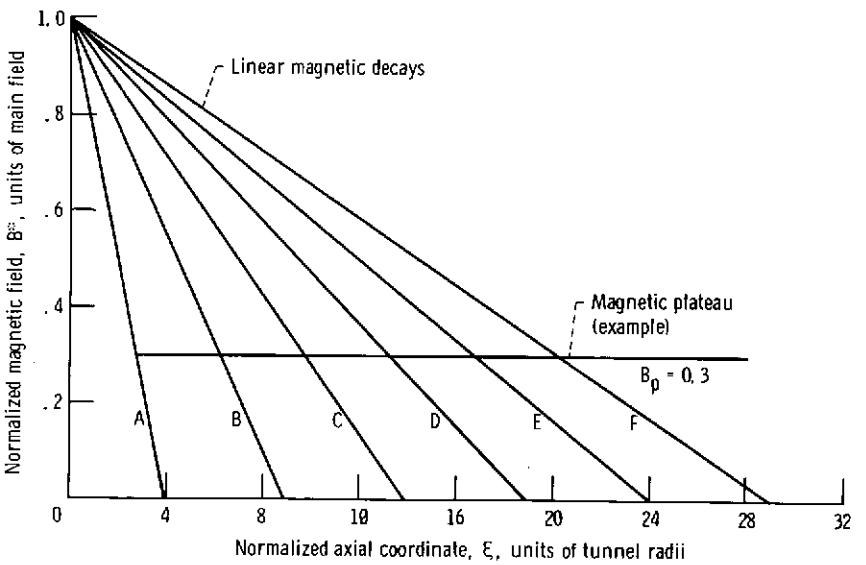

Figure 2. - Magnetic configurations.

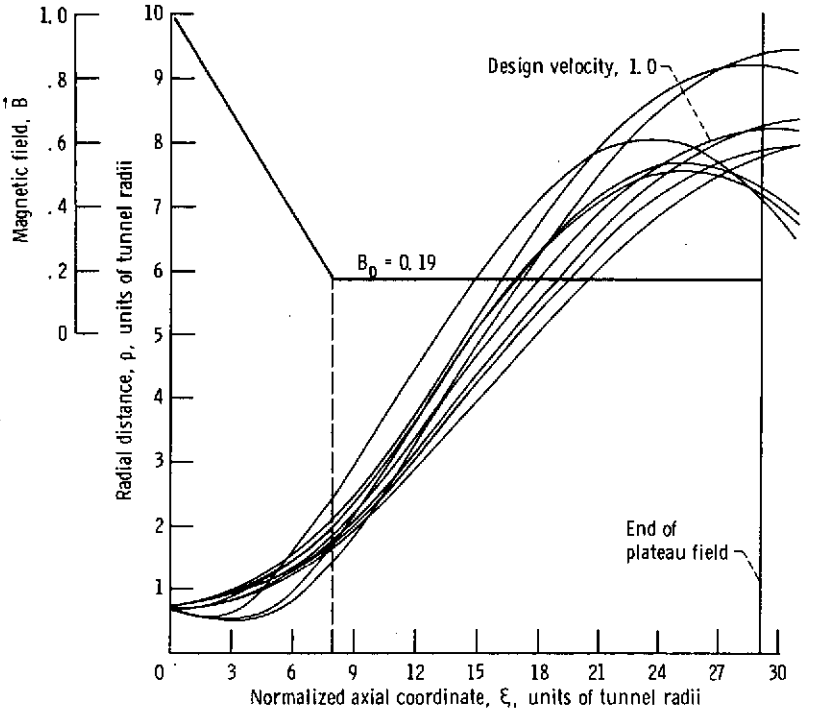

Figure 3. - Typical electron trajectories within refocusing region.

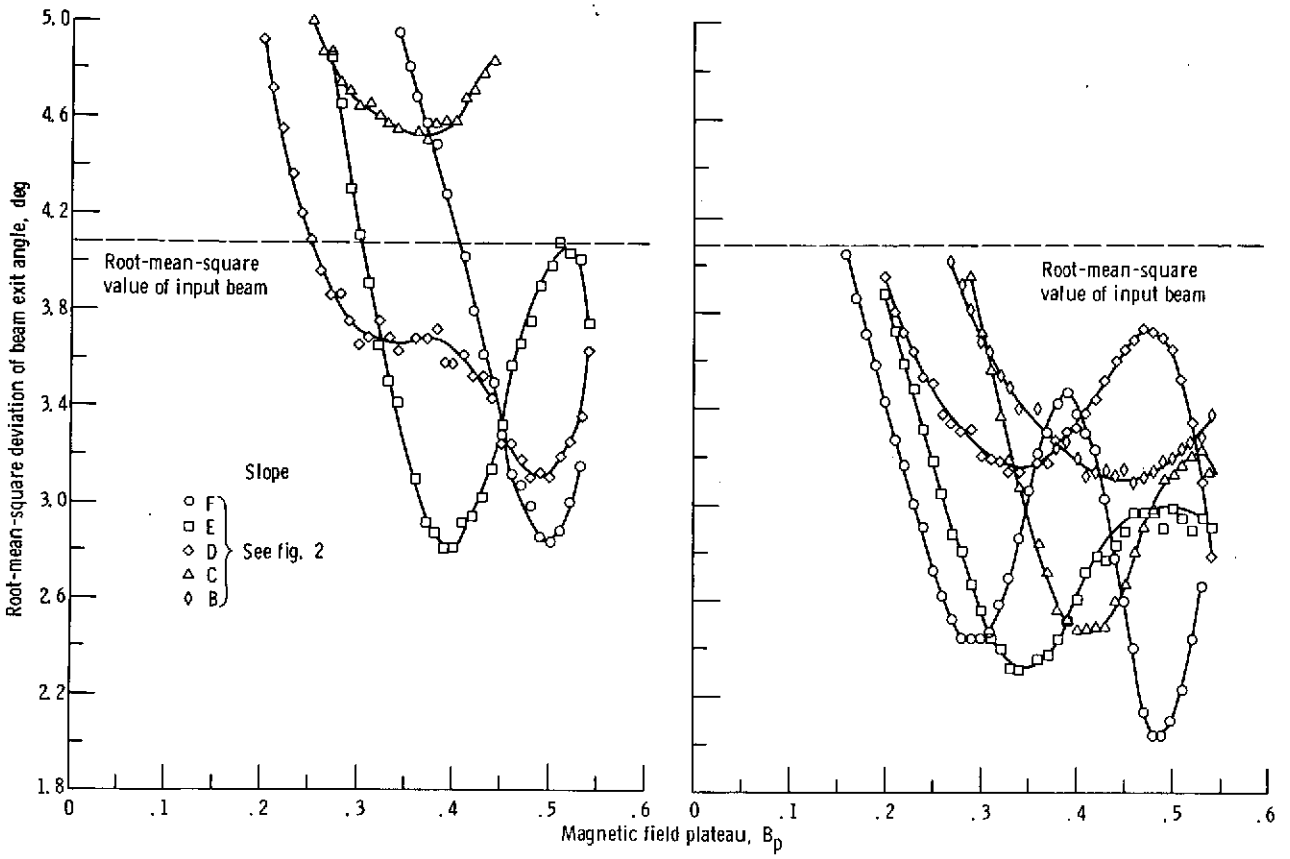

(a) Cathode field, 0.1; plateau design field, 1.0.

(b) Cathode field, 0.9; plateau design field, 1.0.

Figure 4. - Root-mean-square deviation of exit angles as function of magnetic field plateau for various decay slopes.

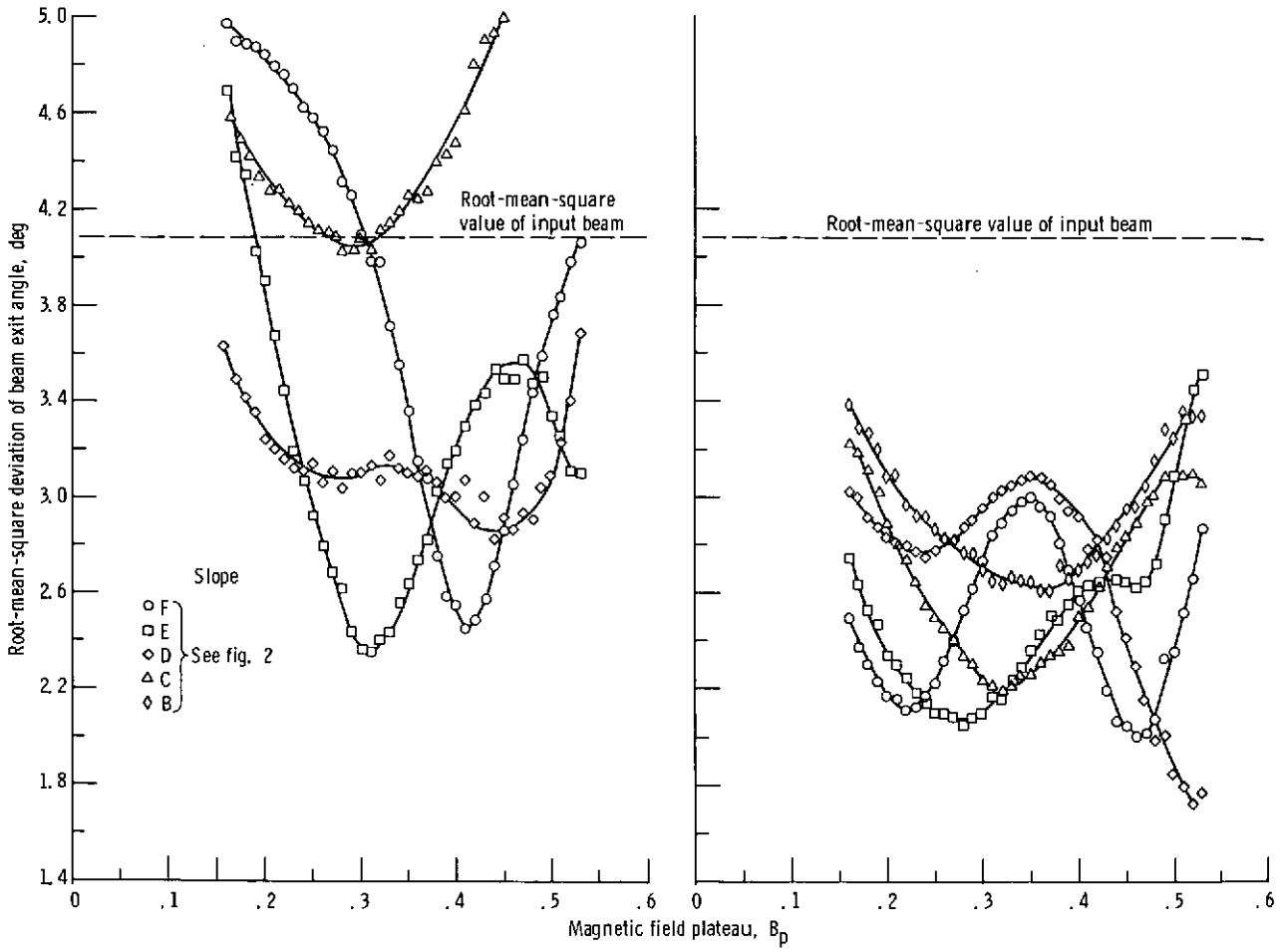

(c) Cathode field, 0.1; plateau design velocity, 0.7.

(d) Cathode field, 0.9; plateau design velocity, 0.7.

Figure 4. - Concluded.

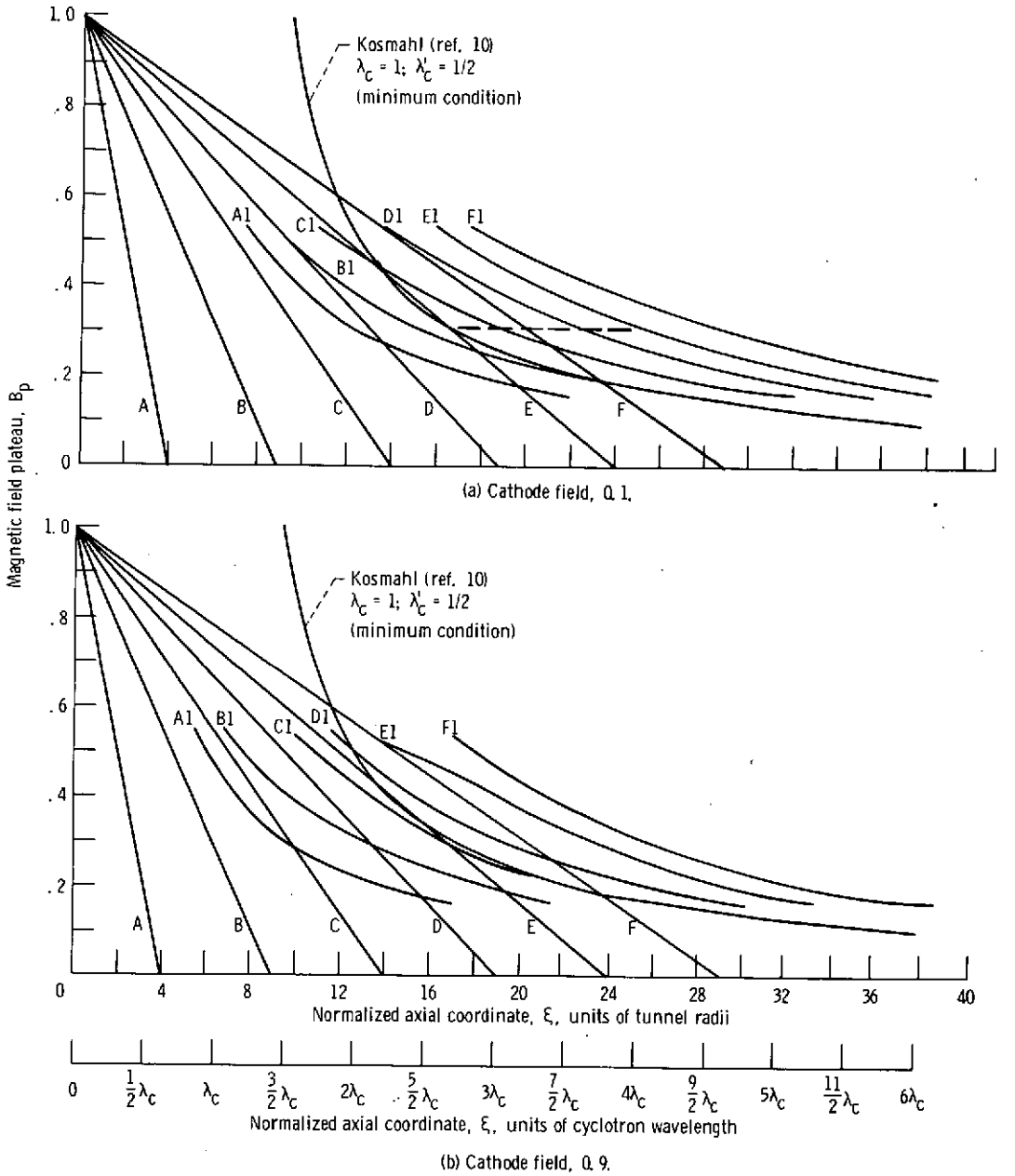

Figure 5. - Magnetic field plateau as function of axial distance for various decay slopes. Plateau design velocity, 0.7.

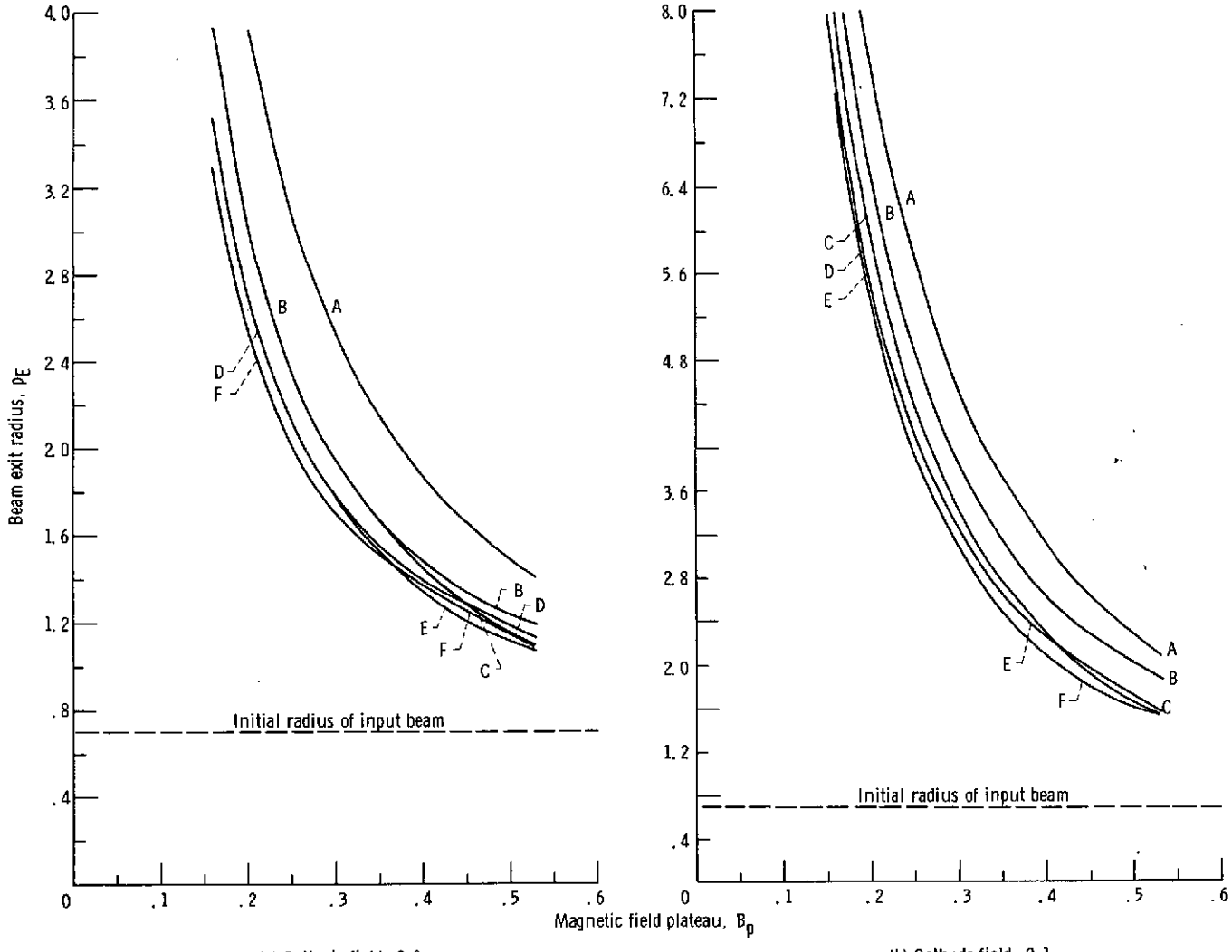

(a) Cathode field, 0.9.

(b) Cathode field, 0.1.

Figure 6. - Beam radius at exit as function of magnetic field plateau for various decay slopes. Plateau design velocity, 0.7.